Prediction of Attractive Level Crossing via a Dissipative Mode

Weichao Yu (余伟超),[1,2] Jiongjie Wang,[1] H. Y. Yuan,[3] and Jiang Xiao (萧江)[1,4,*]
[1]Department of Physics and State Key Laboratory of Surface Physics, Fudan University, Shanghai 200433, China
[2]Institute for Materials Research, Tohoku University, Sendai 980-8577, Japan
[3]Department of Physics, Southern University of Science and Technology, Shenzhen 518055, Guangdong, China
[4]Institute for Nanoelectronics Devices and Quantum Computing, Fudan University, Shanghai 200433, China

(Received 15 July 2019; revised manuscript received 13 September 2019; published 26 November 2019)

The new field of spin cavitronics focuses on the interaction between the magnon excitation of a magnetic element and the electromagnetic wave in a microwave cavity. In the strong interaction regime, such an interaction usually gives rise to the level anticrossing for the magnonic and the electromagnetic mode. Recently, the attractive level crossing has been observed, and it is explained by a non-Hermitian model Hamiltonian. However, the mechanism of such attractive coupling is still unclear. We reveal the secret by using a simple model with two harmonic oscillators coupled to a third oscillator with large dissipation. We further identify this dissipative third party as the invisible cavity mode with large leakage in cavity-magnon experiments. This understanding enables one to design dissipative coupling in all sorts of coupled systems.

DOI: 10.1103/PhysRevLett.123.227201

Introduction.—Spin cavitronics is a newly developing interdisciplinary field that combines spintronics with cavity quantum electrodynamics, and its purpose is to realize quantum information processing via photon-magnon interaction. The strong interaction between the Kittel mode of a magnetic yttrium iron garnet (YIG) sphere [1] and cavity photons has been observed [2–4], even in the quantum regime [5–7]. The spin cavitronic system provides a platform for interfacing a magnon with a photon. By placing a magnetic element in a cavity, it is possible to convert an optical photon to a microwave photon bidirectionally through ferromagnetic magnons [8], or to transfer spin information between two magnets via cavity photons [9,10]. In the presence of several YIG spheres, the indirect coupling among them can be induced by the cavity photons [11], leading to hybridized magnonic modes [12,13]. These hybrid modes can be interpreted using molecular orbital theory so that the design of magnonic molecules with novel properties is expected [14]. The peculiar dynamics of these modes (bright mode and dark mode) are beneficial for quantum information manipulation and storage [12].

Mode hybridization between the magnon and the photon is no different than any other coupling system, where avoided crossing between the energy levels of two eigenmodes is expected, and the size of the anticrossing gap is proportional to the strength of the coupling. However, Grigoryan *et al.* [15] proposed that an attractive level crossing can be realized via artificial coupling using an external feedback circuit, which was recently demonstrated experimentally [16]. Recent experiments have also observed attractive level crossings of different physical origins in a Fabry-Perot-like cavity [17] and in coplanar-waveguide-based resonator structures [18,19]. Model Hamiltonians with non-Hermitian dissipative terms have been proposed to interpret the experiments [20]. Such mathematical constructions, however, lack a physical explanation or mechanism, leaving the level-attraction behavior in such systems yet to be understood.

In this Letter, we reduce the seemingly complicated cavity-magnon system into an extremely simple model with two coupled harmonic oscillators, where the mutual coupling forces are proportional to (i) their position difference (equivalent to a normal spring) or (ii) their velocity difference (no conventional analogy). It can be shown that the type (i) coupling is reactive and gives rise to the usual repulsive level crossing, while the type (ii) coupling is dissipative and leads to the attractive level crossing. The main contribution of this Letter is to show that, in a physical system, the dissipative type (ii) coupling can be realized by coupling both oscillators reactively to a third highly dissipative entity. We further identify the third-party mode in the level-attraction experiments in cavity systems as the invisible cavity mode with extremely high leakage or dissipation. Interestingly, the physical mechanism for level attraction in coupled oscillators discussed in this Letter can also explain the mystery of the centuries old Huygens clock synchronization problem [21].

The oscillator model.—Let us consider the simplest coupled harmonic oscillator model, as shown in Fig. 1(a). The two oscillators may refer to any physical eigenmodes, and for the present interest in spin cavitronics, they can be understood as the cavity photon mode and the Kittel magnon mode in the YIG sphere. Let ω_i, η_i be the resonance frequency and damping constant for oscillator i ($i = 1, 2$). The dynamics of displacements $x_{i=1,2}$ are described as coupled damped oscillators ($i' \equiv 3 - i$):

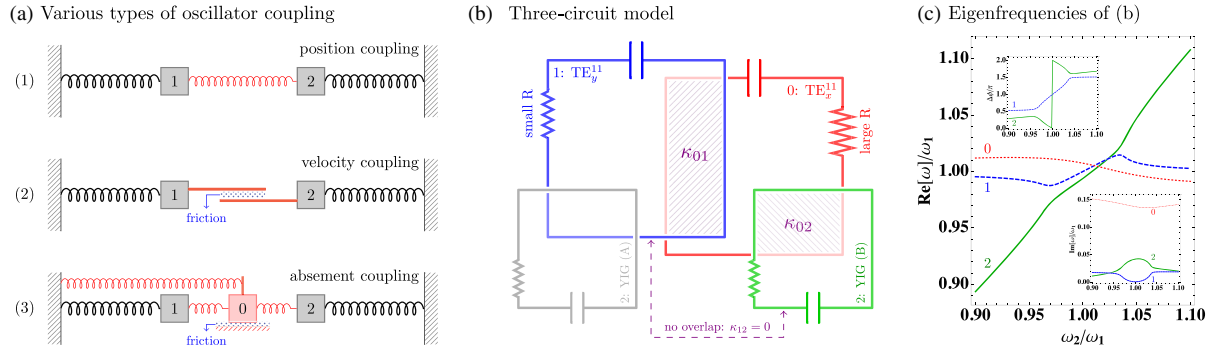

FIG. 1. (a)(1) Harmonic oscillators with reactive coupling via a direct spring, (a)(2) dissipative coupling via viscous forces, and (a)(3) dissipative coupling via a third oscillator m_0 in contact with the friction surface. (b) The three-circuit model with three RLC circuits. Both circuit 1 (blue) and circuit 2 (green) are coupled reactively to a highly dissipative third party, circuit 3 (red), realizing dissipative coupling between circuits 1 and 2. The circuits 0, 1, 2 here are equivalent to the high dissipative TE_x^{11} mode, the low dissipative cavity TE_y^{11} mode, and the YIG magnon mode in Fig. 4. (c) The eigenfrequencies for the three-circuit model with $\omega_0=\omega_1$, $\lambda_i=1$, $\kappa_{12}=0$, $\kappa_{0i}=0.11$, $\gamma_0/\omega_1=0.35$, and $\gamma_1/\omega_1=\gamma_2/2\omega_1=0.001$. (Insets) The imaginary part of the eigenfrequencies (bottom panel) and the relative phase (top panel) between circuits 1 and 2.

$$\ddot{x}_i+\omega_i^2 x_i+\eta_i\dot{x}_i=\kappa_i\hat{T}(x_{i'}-x_i). \tag{1}$$

The terms on the right-hand side represent generic coupling forces, which are related to the relative displacement x_2-x_1 via an operator $\hat{T}$ and are characterized by strength κ_i. The exact nature of the coupling is represented by the operator $\hat{T}$. For example, for $\hat{T}=\hat{T}_0=1$, the coupling can be simply realized by a spring connecting the two oscillators as in Fig. 1(a)(1); i.e., the mutual force depends on their relative displacement. If $\hat{T}=\hat{T}_1=d/dt$ is the time derivative operator, then the mutual force is proportional to their relative velocity, which can be realized via viscous force between the two oscillators as in Fig. 1(a)(2). When $\hat{T}=\hat{T}_{-1}=\int dt$ is the temporal integration operator, the coupling force is proportional to the relative absement (the time integral of displacement), which can be realized via a third oscillator with extra dissipation as in Fig. 1(a)(3). In general, we may define $\hat{T}_n\equiv d^n/dt^n$ and $\hat{T}_{-n}\equiv\int d^n t$. Since, for an even n, $\hat{T}_n$ are even under time reversal, they will lead to reactive coupling, while, for an odd n, $\hat{T}_n$ are odd under time reversal; therefore, they represent dissipative coupling. Solving Eq. (1) by assuming the harmonic ansatz $x_i(t)=\tilde{x}_i e^{i\omega t}$, we find that the energy levels (see the Supplemental Material [22]) show the usual repulsive anticrossing for the reactive coupling $\hat{T}_0$, but an attractive level crossing for the velocity or absement couplings $\hat{T}_{\pm1}$. One example of velocity coupling has been proposed in a spintronic system where two ferromagnetic layers are coupled via spin pumping and spin-transfer torque [23], where the spin current pumped from one magnet acts as spin-transfer torque on the other magnet, resulting in level attraction or synchronization. Note that the Rayleigh dissipation matrix of the system with velocity coupling is always non-negative, which is similar to that of a two-sublattice antiferromagnet, and thus guarantees the second law of thermal dynamics [24].

The three-circuit model.—To better capture the physics in the cavity-magnon system, we construct a model system consisting of three mutually overlapping RLC circuits, as shown in Fig. 1(b), equivalent to the previous three-oscillator model. The coupling between the RLC circuits are realized via the mutual inductance and the coupling strength $\kappa_{ij}=\kappa_{ji}$ between circuit i and circuit j is proportional to the area of their overlapping region. Letting the resistance, inductance, and capacitance be denoted by $R_{0,1,2}$, $L_{0,1,2}$, and $C_{0,1,2}$, respectively, the currents $I_{i=1,2}$ and I_0 in the three circuits satisfy

$$\ddot{I}_i+\omega_i^2 I_i=-\gamma_i\dot{I}_i+\kappa_{ii'}\ddot{I}_{i'}+\frac{\kappa_{0i}}{\lambda_i}\ddot{I}_0, \tag{2a}$$

$$\ddot{I}_0+\omega_0^2 I_0=-\gamma_0\dot{I}_0+\sum_{j=1,2}\lambda_j\kappa_{0j}\ddot{I}_j, \tag{2b}$$

where $\omega_i=1/\sqrt{L_iC_i}$, $\gamma_i=R_i/L_i$, $\lambda_i=L_i/L_0$. The $\ddot{I}_{i'}$ term in Eq. (2a) is the direct coupling between circuits 1 and 2, which is the even (reactive) $\hat{T}_2$ type coupling.

When circuit 0 has small dissipation (small γ_0), the realized coupling between circuits 1 and 2 is conventional repulsive coupling. However, we shall see below that, if the dissipation of circuit 0 is large, the effective coupling between circuits 1 and 2 becomes dissipative attractive coupling. To see this point, let us take a limiting case with the left-hand side of Eq. (2b) neglected, then $\ddot{I}_0$ can be replaced by $\ddot{I}_{1,2}\sim\hat{T}_3 I_{1,2}$, and Eq. (2a) becomes

$$\ddot{I}_i+\omega_i^2 I_i+\gamma_i\dot{I}_i-\frac{\kappa_{0i}^2}{\gamma_0}I_i=\left(\kappa_{12}\hat{T}_2+\frac{\kappa_{01}\kappa_{02}}{\gamma_0}\frac{\lambda_{i'}}{\lambda_i}\hat{T}_3\right)I_{i'}, \tag{3}$$

where the right-hand side contains both reactive ($\hat{T}_2$) and dissipative ($\hat{T}_3$) couplings. If $\kappa_{12} = 0$ (no overlap between circuits 1 and 2), the reactive coupling is turned off, and the dissipative coupling dominates. The neglect of the left-hand side of Eq. (2b) can be achieved when circuit 0 oscillates at a frequency close to the resonance frequency $\omega_0 \simeq \omega$, and the dissipation γ_0 is larger than the detuning $\gamma_0\omega \gg |\omega^2 - \omega_0^2|$ [25]. Therefore, to enhance the dissipative coupling (governed by the prefactor of $\hat{T}_3$), one needs to have the third-party dissipation γ_0 being as small as possible, yet large enough that $\gamma_0\omega \gg |\omega^2 - \omega_0^2|$. Figure 1(c) shows such attractive coupling realized in the three-circuit model in the regime described above. Moreover, modes 1 and 2 have roughly an equal amount of energy in the level-attraction region.

The three-mode quantum model.—In a quantum description, using the annihilation operator $\hat{a}_j$ for mode j ($j = 0$, 1, 2), the system Hamiltonian for three coupled modes can be written as

$$\hat{H} = \sum_{j=0,1,2} \hbar\omega_j \hat{a}_j^\dagger \hat{a}_j + \sum_{j<k} \kappa_{jk}(\hat{a}_j^\dagger \hat{a}_k + \hat{a}_k^\dagger \hat{a}_j)$$
$$= \begin{pmatrix} \omega_1 & \kappa_{12} & \kappa_{01} \\ \kappa_{12} & \omega_2 & \kappa_{02} \\ \kappa_{01} & \kappa_{02} & \omega_0 \end{pmatrix} \rightarrow \hat{U}^\dagger \hat{H}\, \hat{U} = \begin{pmatrix} \omega_1' & \kappa_{12}' & 0 \\ \kappa_{12}' & \omega_2' & 0 \\ 0 & 0 & \omega_0' \end{pmatrix}.$$

Without loss of generality, we can assume that $\kappa_{ij} = \kappa_{ji}$ are real. This Hamiltonian becomes non-Hermitian if we allow the eigenfrequencies to have both real and imaginary components: $\omega_j = \omega_j^r - i\gamma_j$. Since we are interested in the subsystem with modes 1 and 2, we can transform away their coupling with mode 0 from the Hamiltonian. This is equivalent to performing a unitary transformation $\hat{U}$ to block diagonalize the three-mode system into the decoupled two-mode and one-mode subsystems as above. When the coupling with the mode 0 is weak, such a transformation can be realized using the Schrieffer-Wolff transformation [26] (see the Supplemental Material [22]), and the resulting effective coupling between modes 1 and 2 and the renormalized eigenfrequencies are

$$\kappa_{12}' = \kappa_{12} + \frac{1}{2}\kappa_{01}\kappa_{02} \sum_{i=1,2} \frac{1}{\omega_i^r - \omega_0^r - i(\gamma_i - \gamma_0)}, \tag{5a}$$

$$\omega_i' = \omega_i^r - i\gamma_i + \frac{\kappa_{0i}^2}{\omega_i^r - \omega_0^r - i(\gamma_i - \gamma_0)}. \tag{5b}$$

The decoupling of the third dissipative mode, mode 0, effectively renormalizes the coupling ($\kappa_{12} \rightarrow \kappa_{12}'$) between modes 1 and 2 and modifies their eigenfrequencies with the additional dissipation ($\omega_i \rightarrow \omega_i'$). And the latter guarantees the non-negativeness of the dissipation of the model. When the direct coupling vanishes ($\kappa_{12} = 0$), the effective coupling κ_{12}' becomes imaginary when $|\omega_i^r - \omega_0^r| \ll |\gamma_i - \gamma_0|$, and this is realized when mode 0 has large dissipation (γ_0). This condition is the same as that in the classical model in Eq. (3); i.e., the γ_0 should be large such that $\omega_i - \omega_0$ is dominated by γ_0, but not so large such that the coupling strength (κ_{12}') is still sizable.

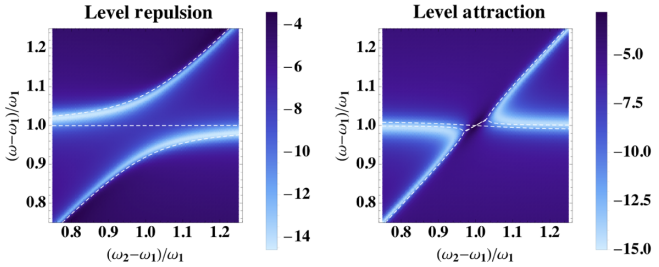

FIG. 2. Transmission spectra S_{21} calculated from input-output theory. (Left panel) Direct coupling between modes 1 and 2 ($\kappa_{12,10} \neq 0$, $\kappa_{20} = 0$) gives rise to repulsive coupling. (Right panel) Indirect coupling between modes 1 and 2 via dissipative mode 0 ($\kappa_{10,20} \neq 0$, $\kappa_{12} = 0$) leads to attractive coupling (see the Supplemental Material [22] for calculation details and parameters). The color scale is in decibels using $10\log|S_{21}|^2$. The white dashed lines are the eigenfrequencies calculated directly from the three-mode Hamiltonian (4).

Based on the three-mode quantum model, we also calculate the transmission spectrum based on standard input-output theory [27] (see the Supplemental Material [22]). Figure 2 shows that the transmission spectra and the eigenvalues calculated solely from the Hamiltonian agree very well, and they both show that level attraction appears when modes 1 and 2 are coupled via a dissipative mode 0.

Level attraction in a directional coupler.—To illustrate the attractive coupling principle more clearly, we demonstrate the attractive behavior in a directional coupler using finite-element simulation [28] (see the Supplemental Material [22]). A coupled-transmission-line directional coupler, as shown in Fig. 3(a), consists of two parallel metal stripes on a dielectric substrate. The lower stripe (working as a waveguide) is connected with input and output ports. When the microwave travels through the lower stripe, it partially leaks (couples) to the upper stripe (the cavity), exciting the cavity modes of the upper stripe, which can be detected via the transmission spectrum.

Unlike the circular or cross cavity used in Refs. [17,19], the cavity and the dissipative mode in a directional coupler are spatially separated, which enables us to see the coupling more clearly. Let us focus on the cavity mode at $f =$ 9.16 GHz. Figure 3(a) shows the spatial distribution of the in-plane magnetic field of this mode over a plane slightly beneath the metal stripes. The cavity mode in the upper stripe has a vanishing magnetic field at the edges and at the center of the stripe. While the dissipative mode in the lower stripe has its maximum magnetic field at the edges and at the center, which has a quarter wavelength offset from the cavity mode. This offset between the cavity and

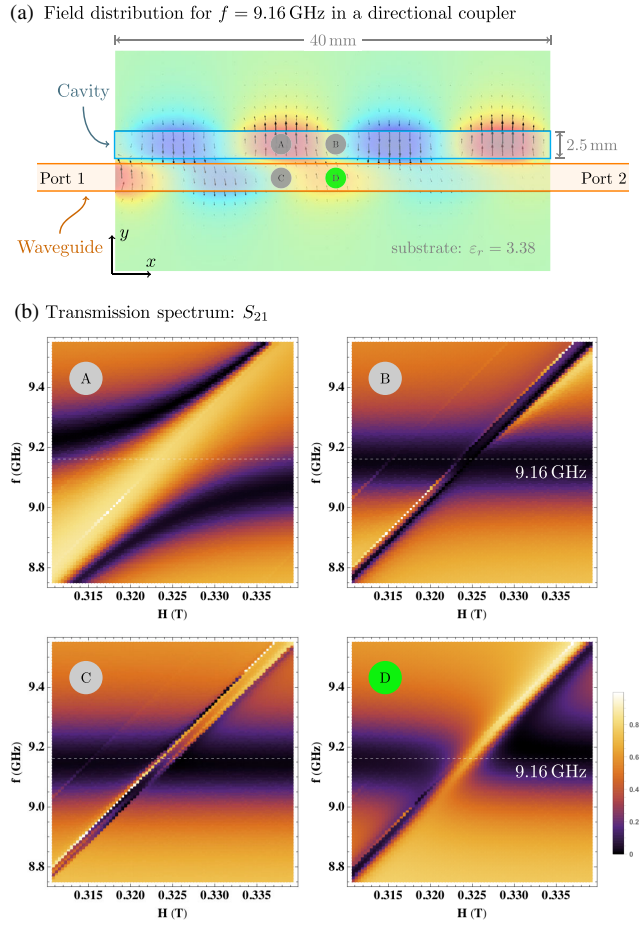

FIG. 3. (a) The magnetic field distribution for the $f = 9.16$ GHz cavity mode in a directional coupler with the microwaves injected from port 1. The length of the coupler is 40 mm, the width of each stripe is 2.5 mm, and the relative dielectric constant of the substrate is $\varepsilon_r = 3.38$. (b) The simulated transmission spectrum when the YIG sphere is placed at points A, B, C, D, respectively. All material parameters are the same as those in Ref. [19].

the dissipative mode means that the locations with the maximum magnetic field for the cavity mode correspond to the spots of zero magnetic field for the dissipative mode, and vice versa.

We now study the transmission spectrums when the YIG sphere (with diameter 1 mm) is placed 0.75 mm beneath the metal stripe and at four different locations, A, B, C, D. Point A is the magnetic field antinode (of maximum field) for the cavity mode; therefore, the YIG sphere is coupled to the cavity directly, resulting in the conventional repulsive coupling [see panel A in 3(b)], while points B and C are on the magnetic field nodes (of zero or negligible field) for the cavity and the dissipative modes. Thus no coupling is observed [panels B and C in Fig. 3(b)]. Point D, however, is the magnetic field node for the cavity mode, but the antinode for the dissipative mode; therefore, the YIG sphere is coupled only to the dissipative mode—not to

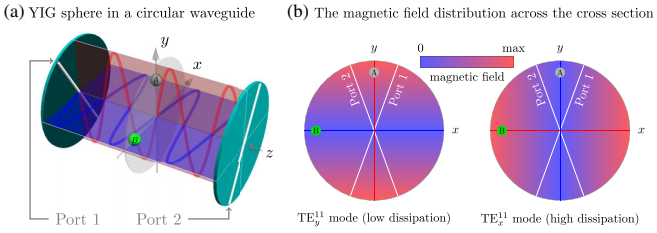

FIG. 4. (a) YIG sphere in a circular waveguide. (b) The magnetic field distribution across the cross section. The magnetic field vanishes along $\hat{\mathbf{x}}$ for the cavity TE_y^{11} mode (left panel) and vanishes along $\hat{\mathbf{y}}$ for the TE_x^{11} mode (right panel). When the YIG sphere is placed at point A (B), it couples strongly with TE_x^{11} (TE_y^{11}) mode.

the cavity mode. Considering that the cavity mode is also coupled to the dissipative mode along the path, the scenario of YIG and the cavity modes coupled via a third dissipative mode is realized, leading to an attractive level crossing, as shown in panel D of Fig. 3(b).

Interpretation of the level attraction in the circular waveguide.—In the circular cavity–YIG system [schematically illustrated in Fig. 4(a)] studied in Ref. [17], the repulsive and attractive level crossings are observed when the YIG sphere is placed at points A and B, which correspond to the magnetic field antinode and node for the cavity mode, respectively. We shall be clear below that the cavity and the YIG mode realize attractive level crossing via their coupling to a common dissipative third party, just as in the cases studied above. The issue is, what is the third party in the circular cavity? To answer that, we note that the circular cavity of interest has two ports, forming a small angle [see Fig. 4(a)]. These ports play two roles: (i) they are used for feeding and draining the TE electromagnetic wave into and out of the cavity, and (ii) they reflect TE waves polarized perpendicular to the port orientations. If there were no ports, the cavity should have electromagnetic (EM) modes of all polarizations. However, because of the opening ports, the cavity mode with polarization along $\hat{\mathbf{y}}$ (call it TE_y^{11}) has the longest lifetime. The EM mode polarized along $\hat{\mathbf{x}}$ (TE_x^{11}) has the largest leakage through the two ports, and thus the shortest lifetime. The long-lived TE_y^{11} mode is the visible cavity mode we usually measure, and its magnetic field (anti)node is along $\hat{\mathbf{x}}$ ($\hat{\mathbf{y}}$) [see Fig. 4(b)]. The TE_x^{11} mode is invisible due to its extremely short lifetime, and its magnetic field (anti)node is the opposite of that of the TE_y^{11} mode [see Fig. 4(b)]. Therefore, when the YIG sphere is placed at point B, it is coupled not to the cavity mode TE_y^{11} but to the dissipative TE_x^{11} mode. In addition, the TE_x^{11} and TE_y^{11} modes are coupled through multiple reflections by the ports. Consequently, the TE_x^{11} works as the dissipative third party that couples the cavity TE_y^{11} mode to the YIG magnon mode, leading to their attractive level crossing, as observed in the experiment.

The high-dissipation TE_x^{11} mode satisfies the requirement for working as the third party: the TE_x^{11} mode has the same eigenfrequency as the cavity TE_y^{11} mode, so $\omega_0 \simeq \omega_1$ is very close to the resonant frequency ω. This minimizes $|\omega^2 - \omega_0^2|$. Because the TE_x^{11} mode has high leakage through the ports (and thus large γ_0), $\gamma_0\omega \gg |\omega^2 - \omega_0^2|$ is naturally satisfied.

Discussion and conclusion.—The level attraction via a dissipative mode is a general physical principle, which can be applied to a wide range of coupled physical systems. For example, either the oscillator or the dissipative third party can be a superconducting qubit [6,29], a dielectric nanostructure [30], an antiferromagnet [31,32], a high-order spin wave mode [33], or another excitation such as a phonon [34]. It has been reported recently that magnetic textures can also be coupled with the cavity photons [35,36]. Based on the understanding of dissipative coupling, the nonlinear effect [37,38] and topological properties of the exceptional point [39–42] can be generalized, and new physics is expected.

In conclusion, we found that the mechanism for the dissipative coupling in many physical systems can be captured by an effective three-oscillator model, where two oscillators of interests are coupled to a common third oscillator with strong dissipation. We verify this model in both classical and quantum setups. Based on this model, we are able to explain the exact physical mechanisms behind the level-attraction experiments carried out in cavity-magnon systems, where a hidden cavity mode with large dissipation is responsible for mediating the dissipative coupling.

This work was supported by the National Natural Science Foundation of China (Grants No. 11722430, No. 11847202, and No. 61704071). W. Y. is also supported by the China Postdoctoral Science Foundation under Grant No. 2018M641906. J. X. is also supported by the Shuguang Program of the Shanghai Education Development Foundation and the Shanghai Municipal Education Commission.

*Corresponding author.
xiaojiang@fudan.edu.cn

[1] C. Kittel, Phys. Rev. **73**, 155 (1948).
[2] Ö. O. Soykal and M. E. Flatté, Phys. Rev. Lett. **104**, 077202 (2010).
[3] H. Huebl, C. W. Zollitsch, J. Lotze, F. Hocke, M. Greifenstein, A. Marx, R. Gross, and S. T. B. Goennenwein, Phys. Rev. Lett. **111**, 127003 (2013).
[4] X. Zhang, C.-L. Zou, L. Jiang, and H. X. Tang, Phys. Rev. Lett. **113**, 156401 (2014).
[5] Y. Tabuchi, S. Ishino, T. Ishikawa, R. Yamazaki, K. Usami, and Y. Nakamura, Phys. Rev. Lett. **113**, 083603 (2014).
[6] D. Lachance-Quirion, Y. Tabuchi, S. Ishino, A. Noguchi, T. Ishikawa, R. Yamazaki, and Y. Nakamura, Sci. Adv. **3**, e1603150 (2017).
[7] Y. Tabuchi, S. Ishino, A. Noguchi, T. Ishikawa, R. Yamazaki, K. Usami, and Y. Nakamura, C.R. Phys. **17**, 729 (2016).
[8] R. Hisatomi, A. Osada, Y. Tabuchi, T. Ishikawa, A. Noguchi, R. Yamazaki, K. Usami, and Y. Nakamura, Phys. Rev. B **93**, 174427 (2016).
[9] L. Bai, M. Harder, Y. P. Chen, X. Fan, J. Q. Xiao, and C.-M. Hu, Phys. Rev. Lett. **114**, 227201 (2015).
[10] L. Bai, M. Harder, P. Hyde, Z. Zhang, C.-M. Hu, Y. P. Chen, and J. Q. Xiao, Phys. Rev. Lett. **118**, 217201 (2017).
[11] N. J. Lambert, J. A. Haigh, S. Langenfeld, A. C. Doherty, and A. J. Ferguson, Phys. Rev. A **93**, 021803(R) (2016).
[12] X. Zhang, C.-L. Zou, N. Zhu, F. Marquardt, L. Jiang, and H. X. Tang, Nat. Commun. **6**, 8914 (2015).
[13] Y. Xiao, X. H. Yan, Y. Zhang, V. L. Grigoryan, C. M. Hu, H. Guo, and K. Xia, Phys. Rev. B **99**, 094407 (2019).
[14] B. Zare Rameshti and G. E. W. Bauer, Phys. Rev. B **97**, 014419 (2018).
[15] V. L. Grigoryan, K. Shen, and K. Xia, Phys. Rev. B **98**, 024406 (2018).
[16] I. Boventer, C. Dörflinger, T. Wolz, R. Macêdo, R. Lebrun, M. Kläui, and M. Weides, arXiv:1904.00393.
[17] M. Harder, Y. Yang, B. M. Yao, C. H. Yu, J. W. Rao, Y. S. Gui, R. L. Stamps, and C.-M. Hu, Phys. Rev. Lett. **121**, 137203 (2018).
[18] B. Bhoi, B. Kim, S.-H. Jang, J. Kim, J. Yang, Y.-J. Cho, and S.-K. Kim, Phys. Rev. B **99**, 134426 (2019).
[19] Y. Yang, J. W. Rao, Y. S. Gui, B. M. Yao, W. Lu, and C.-M. Hu, Phys. Rev. Applied **11**, 054023 (2019).
[20] B. Yao, T. Yu, X. Zhang, W. Lu, Y. Gui, C.-M. Hu, and Y. M. Blanter, arXiv:1906.12142.
[21] M. Bennett, M. F. Schatz, H. Rockwood, and K. Wiesenfeld, Proc. R. Soc. A **458**, 563 (2002).
[22] See Supplemental Material at http://link.aps.org/supplemental/10.1103/PhysRevLett.123.227201 for derivation of the effective Hamiltonian, details of numerical method and input-output formalism for the three-mode quantum model.
[23] B. Heinrich, Y. Tserkovnyak, G. Woltersdorf, A. Brataas, R. Urban, and G. E. W. Bauer, Phys. Rev. Lett. **90**, 187601 (2003).
[24] H. Y. Yuan, Q. Liu, K. Xia, Z. Yuan, and X. R. Wang, Europhys. Lett. **126**, 67006 (2019).
[25] Another condition for the negligible left-hand side of Eq. (2b) is to let $L_0 \to 0$ and $C_0 \to \infty$ so that $\gamma_0 \dot{I}_0$ dominates Eq. (2b).
[26] J. R. Schrieffer and P. A. Wolff, Phys. Rev. **149**, 491 (1966).
[27] D. F. Walls and G. J. Milburn, *Quantum Optics* (Springer Science+Business Media, New York, 2007).
[28] Computer code COMSOL Multiphysics,® version 5.4, http://www.comsol.com.
[29] Y. Tabuchi, S. Ishino, A. Noguchi, T. Ishikawa, R. Yamazaki, K. Usami, and Y. Nakamura, Science **349**, 405 (2015).
[30] T. C. Preston and R. Signorell, Proc. Natl. Acad. Sci. U.S.A. **108**, 5532 (2011).
[31] O. Johansen and A. Brataas, Phys. Rev. Lett. **121**, 087204 (2018).

[32] H. Y. Yuan and X. R. Wang, Appl. Phys. Lett. **110**, 082403 (2017).
[33] Y. Cao, P. Yan, H. Huebl, S. T. B. Goennenwein, and G. E. W. Bauer, Phys. Rev. B **91**, 094423 (2015).
[34] X. Zhang, C.-L. Zou, L. Jiang, and H. X. Tang, Sci. Adv. **2**, e1501286 (2016).
[35] I. Proskurin, A. S. Ovchinnikov, J.-I. Kishine, and R. L. Stamps, Phys. Rev. B **98**, 220411(R) (2018).
[36] L. V. Abdurakhimov, S. Khan, N. A. Panjwani, J. D. Breeze, M. Mochizuki, S. Seki, Y. Tokura, J. J. L. Morton, and H. Kurebayashi, Phys. Rev. B **99**, 140401(R) (2019).
[37] Y.-P. Wang, G.-Q. Zhang, D. Zhang, X.-Q. Luo, W. Xiong, S.-P. Wang, T.-F. Li, C.-M. Hu, and J. Q. You, Phys. Rev. B **94**, 224410 (2016).
[38] Y.-P. Wang, G.-Q. Zhang, D. Zhang, T.-F. Li, C.-M. Hu, and J. Q. You, Phys. Rev. Lett. **120**, 057202 (2018).
[39] M. Harder, L. Bai, P. Hyde, and C.-M. Hu, Phys. Rev. B **95**, 214411 (2017).
[40] D. Zhang, X.-Q. Luo, Y.-P. Wang, T.-F. Li, and J. Q. You, Nat. Commun. **8**, 1368 (2017).
[41] G.-Q. Zhang and J. Q. You, Phys. Rev. B **99**, 054404 (2019).
[42] Y. Cao and P. Yan, Phys. Rev. B **99**, 214415 (2019).